



Contents lists available at ScienceDirect

Catalysis Today

journal homepage: www.elsevier.com/locate/cattod



A micropacked-bed multi-reactor system with *in situ* raman analysis for catalyst evaluation

Enhong Cao^a, Gemma Brett^b, Peter J. Miedziak^b, John M. Douthwaite^b, Simon Barrass^a, Paul F. McMillan^{c,d}, Graham J. Hutchings^b, Asterios Gavriilidis^{a,*}

^a Department of Chemical Engineering, University College London, Torrington Place, London WC1E 7JE, UK

^b School of Chemistry, Cardiff University, Main Building, Park Place, Cardiff CF10 3AT, UK

^c Materials Chemistry Centre, University College London, 20 Gordon Street, London WC1H 0AJ, UK

^d Department of Chemistry, University College London, 20 Gordon Street, London WC1H 0AJ, UK

ARTICLE INFO

Article history:

Received 3 November 2015

Received in revised form 26 May 2016

Accepted 1 June 2016

Available online xxx

Keywords:

Multiphase reactor

Microchannel reactor

Alcohol aerobic oxidation

Gold-Palladium catalyst

Bimetallic

Trimetallic catalyst

ABSTRACT

A micropacked-bed multi-reactor platform with integrated portable Raman spectrometer is presented for fast evaluation of catalyst activity and stability for gas/liquid/solid reactions. The silicon-glass microreactor was designed and fabricated so that pockets containing the liquid reaction mixture were created after each packed bed, into which the laser could be directed for Raman spectral acquisition. Using the oxidation of benzyl alcohol as a model reaction, the Raman spectrum was found to be affected both by temperature and by the composition of the multiphase reaction mixture which was related to the reaction conversion. These effects were accounted for by calibrating the Raman spectra at the reaction temperature using mixtures produced by the reactors that were analysed independently by gas chromatography. Fourteen catalysts containing different combinations of Au, Pd and Pt supported on TiO₂ prepared by sol-immobilisation (SI) and standard impregnation (SImp) techniques were tested. The results showed that the activity of the catalysts prepared by SI was overall higher than those prepared by SImp, while the activity sequence followed the same pattern: Pd > AuPd > AuPdPt > PdPt > (Au, Pt, AuPt). The Pd and AuPd catalysts from both SI and SImp were stable in 5-h testing, however, for the PdPt and AuPdPt catalysts prepared by SI deactivation was observed.

© 2016 The Authors. Published by Elsevier B.V. This is an open access article under the CC BY license (<http://creativecommons.org/licenses/by/4.0/>).

1. Introduction

Microreactor technology has become more attractive in chemical synthesis and catalytic process development, since the reduced dimensional scale of microreactors can offer unique advantages including enhanced heat and mass transfer, precise control of reaction temperature, reduced safety risks and low environmental impact over conventional macroscale reactors [1–4]. In the last decades the integration of analytical tools with microstructured reactors has become an attractive approach for online process monitoring [3,5,6], which can provide real-time acquisition of reaction information and offer fast and reliable ways for process development and optimisation. The integration of analytical technology has made microreactors a powerful laboratory tool for reaction and kinetic studies. Among various analytical technologies integrated with miniaturised devices, non-invasive spectroscopic measurements have demonstrated benefits in obtaining not only

information in the reaction fluid but also the state of the solid catalyst present in a microreactor [7–9]. Microreactors, especially those containing flat windows, can be easily integrated with spectroscopic techniques. For studies in heterogeneous catalysis, microreactors have been used in catalyst characterisation by integrating spectroscopic techniques such as Raman spectroscopy [10–13], infrared spectroscopy [14,15], X-ray diffraction (XRD) [16,17] and X-ray absorption spectroscopy (XAS) [17–19], providing novel means to investigate catalysts under realistic reaction conditions.

In heterogeneous catalysis, catalyst development is a time-consuming and costly process. Application of high throughput experimentation techniques promises a significant improvement through minimisation of development time and cost [20–22]. High throughput research can be commonly differentiated between primary and secondary screening. Primary screening employs a large number of experiments that are qualitative or semi-quantitative, characterized by very high throughput and is often focused on discoveries of lead catalysts. Secondary screening, which collects more quantitative reaction information for a group of leads, facilitates the further elimination of less effective candidates in the group

* Corresponding author.

E-mail address: a.gavriilidis@ucl.ac.uk (A. Gavriilidis).

<http://dx.doi.org/10.1016/j.cattod.2016.06.007>

0920-5861/© 2016 The Authors. Published by Elsevier B.V. This is an open access article under the CC BY license (<http://creativecommons.org/licenses/by/4.0/>).

and provides information on kinetics and deactivation for process design. The principle of high throughput experimentation is based on a parallelization strategy that increases the research loading without subsequently increasing development time [23,24]. Focusing on the secondary screening stage, this paper presents development of a microreactor-based parallel catalyst testing system for catalytic gas-liquid-solid reactions, which are typically more demanding than gas phase ones.

The incorporation of vibrational spectroscopic techniques, such as FT-IR imaging and Raman, in parallel operando mode can provide a new approach for accelerated fundamental catalyst research under realistic conditions [25–27]. In our previous work, we demonstrated the successful integration of a silicon-glass microreactor with Raman microspectrometry [10] and X-ray absorption spectroscopy [18] for operando/in situ studies of silver catalysed gas phase methanol oxidation to formaldehyde. In a later study of the gas-liquid oxidation of benzyl alcohol on a AuPd/TiO₂ catalyst, our initial goal to identify reaction intermediates on the catalyst surface using Raman spectroscopy was not possible due to the strongly interfering background fluorescence signal originating from the catalyst surface covered with thin layer of liquid [11]. However, the reaction product benzaldehyde could be determined from Raman spectra obtained by focusing the laser inside “liquid pockets” that formed within the packed bed. This method can be used for monitoring the reaction process taking place in a micro-packed bed and relate it to the catalyst activity. This analysis takes only 1–2 s by comparison to conventional GC or HPLC analysis taking typically 15–30 min for one measurement. In the present work we extend this approach to a micropacked-bed multi-reactor system to develop a microreactor platform integrated with an inexpensive portable Raman spectrometer for fast catalyst evaluation.

Au-Pd bimetallic nanoparticles have been proven to be very active for the oxidation of alcohols, and provide high selectivity to aldehydes even under solvent-free reaction conditions [28–31]. However, to achieve high selectivity towards the aldehyde, either a low temperature approach had to be chosen resulting in a low turnover frequency or the conversion was kept at a low level. In recent work reported by He et al., by adding a small amount of Pt metal into the Au-Pd sols, a high selectivity of benzyl alcohol could be achieved in solvent-free oxidation of benzyl alcohol reaction while still preserving high conversion levels [32]. Supported AuPdPt trimetallic catalysts on carbon were synthesized by the sol-immobilization method, together with Au, Pd and Pt monometallic catalysts and AuPd, PdPt and AuPt bimetallic catalysts synthesized for comparative purpose. These catalysts were tested in batch reactor, showing the capability of small amount of Pt in switching-off toluene formation which improves the selectivity towards benzaldehyde [32]. In this work, we now examine the stability and activity of similar catalysts in flow reaction conditions using the developed microreactor platform.

2. Microreactor system design

2.1. Experimental set-up

Fig. 1 shows a schematic diagram of the multi-microreactor platform integrated with a portable Raman spectrometer. The platform consisted of a four-reactor chip assembly, a Ventana-532 Raman spectrometer equipped with fibre optics (Ocean Optics) for data collection and laser excitation, a motorised positioning stage, a gas-liquid supply unit, a set of gas-liquid separators and a temperature controller. The spectrometer uses a 532 nm diode laser for sample excitation. The laser beam is directed into the multichannel reactor and the scattered light is collected using fibre optics optimized for 600 μm diameter and 0.39 NA fibre input. The detector

is a Hamamatsu S11510-1006 back-thinned CCD capable of operating into the near IR range. A single chip design with four parallel micropacked-beds has the advantage of simplifying the system configuration by using one heater, sharing one inlet/outlet connector and easily incorporating the Raman spectrometer optics and positioning stage. The whole set-up was placed in an enclosure in order to avoid interference from room lighting with the Raman signal. The system was designed to allow multiphase (gas-liquid-solid) reactions to be studied at pressures ranging from 1 to 10 bar and temperatures from 25 to 250 °C. Gas and liquid reactants were delivered into the four-reactor chip through four mass flow controllers (MFCs) (SLA mass flow controller, Brooks) and four syringe pumps (Mid pressure module, Cetoni). The effluents from the reactors were collected in a set of four gas-liquid separators where gas and liquid were separated by gravity. The four gas outlets from the separators were directed to a five-port manifold (Upchurch). The combined gas from the five-port manifold passed through a back pressure regulator (BPR, Pressure Tech), which was used to control the pressure of the reactors. The reaction products could be monitored with the on-chip Raman measurement and analysed by offline gas chromatography by collecting the liquid samples from the gas-liquid separators.

2.2. Multi-reactor chip

The portable Ventana Raman spectrometer system produced a 532 nm laser spot with an approximate diameter of 100 μm at the exit from the fibre optic probe. Our previous studies were carried out using a Renishaw micro-Raman system in which the incident beam and scattered light were focused by a microscope objective to approximately 5 μm within a collection cylinder ~8 μm deep, that made it relatively easy to focus the beam inside “liquid pockets” contained within the micropacked bed (with particle size of 50–90 μm) [11]. In the present case, the slightly divergent beam exiting the fibre optic probe that was also used to collect the scattered light had no effective focus and this created initial difficulties in selecting and defining the “liquid pockets” for study and discriminating against background signals. Our initial design of the four channel micropacked-bed reactor thus concentrated on creating a suitable liquid pocket immediately after the catalyst retainer by designing a semi-circular array of Si pillars (20 μm in diameter). This interrupted the gas-liquid flow after the packed bed exit and created a pool of liquid due to capillarity (Fig. 2). An initial chip containing four different arrangements of the pillar group was prepared and tested at gas-liquid flow rates close to those used for the reaction experiments. It can be seen that liquid pockets of sufficient size were formed in Fig. 2a and Fig. 2d, where at least one of the pillar arrays was located close to the catalyst retainer. By placing the pillar arrays further away from the catalyst retainer, only a thin layer of liquid formed along the channel walls (Fig. 2b and c).

Raman spectra were then acquired as a flowing mixture of benzyl alcohol and benzaldehyde (1:1 by volume) and oxygen was passed over the catalyst bed at different liquid and gas flow rates. With the gas-liquid flow patterns shown in Fig. 2b and c, the spectrum was dominated by strong background signals, most likely due to insufficient liquid volume present within the sample excitation/collection volume. However, the liquid pockets formed by the post arrangements shown in Fig. 2a and d produced spectra of sufficient quality for quantitative product analysis (Fig. 3a). As gas-liquid slugs passed next to the liquid pockets, fluctuations of the overall Raman intensities were observed, but these did not affect the overall form of the spectra, and the ratio of areas of peaks at 1700 cm⁻¹ and 1000 cm⁻¹, used to determine the benzaldehyde yield, was not affected to any significant extent (Fig. S1). Fig. 3 also shows spectra acquired by directing the laser on to the bed retainer (Fig. 3b) and on the glass beads bed that was downstream of the cat-

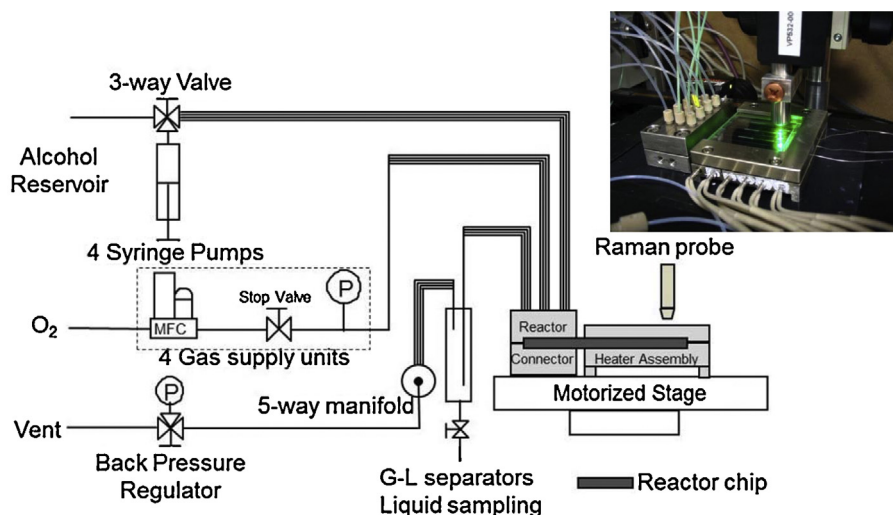


Fig. 1. Schematic diagram of the micro-packed bed multi-microreactor platform. The inset shows a picture of the reactor chip assembly.

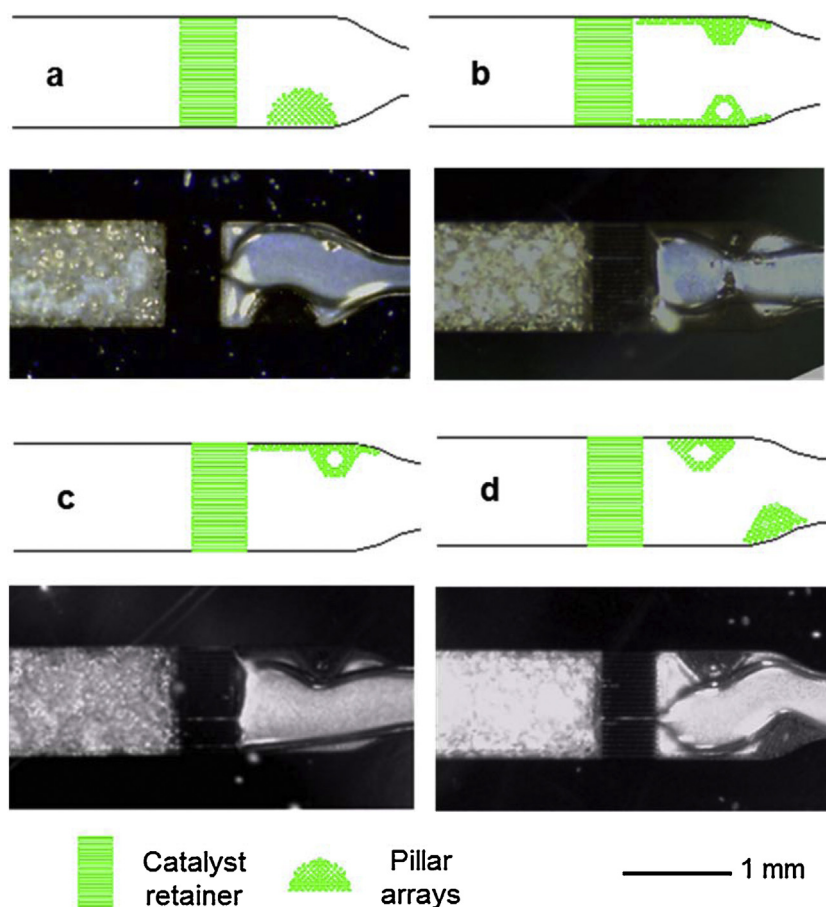


Fig. 2. Catalyst retainer and pillar array structures with the formation of liquid pockets.

alyst bed (Fig. 3c). Only weak peaks were observed due to the lower fraction of liquid sampled within this excitation/collection environment, compounded by light scattering effects from surfaces of bed retainer and glass beads. This part of our work confirms the need for engineering suitable microstructures within the chip to create sufficiently large liquid pockets for online sampling when the fibre optic Raman analysis technique is applied.

Our final design for the reactor chip is shown in Fig. 4a. The four parallel microchannel reactors have independent gas/liquid

inlets and product outlets. The pillar array structure (Fig. 4b) and the liquid pocket during gas/liquid flow over a bed of glass beads (53–63 μm) is also shown (Fig. 4c). The overall size of the reactor chip was 48 mm \times 70 mm. The inlet/outlet ports were arranged at the same end of the reactor chip, while the reaction channels were located towards the other end of the reactor chip. The final design of the semi-circular pillar array after the catalyst retainer was determined by combining the features of the pillar arrays in Fig. 2a and 2d. The width of the reaction channel was 1 mm. The liquid inlet

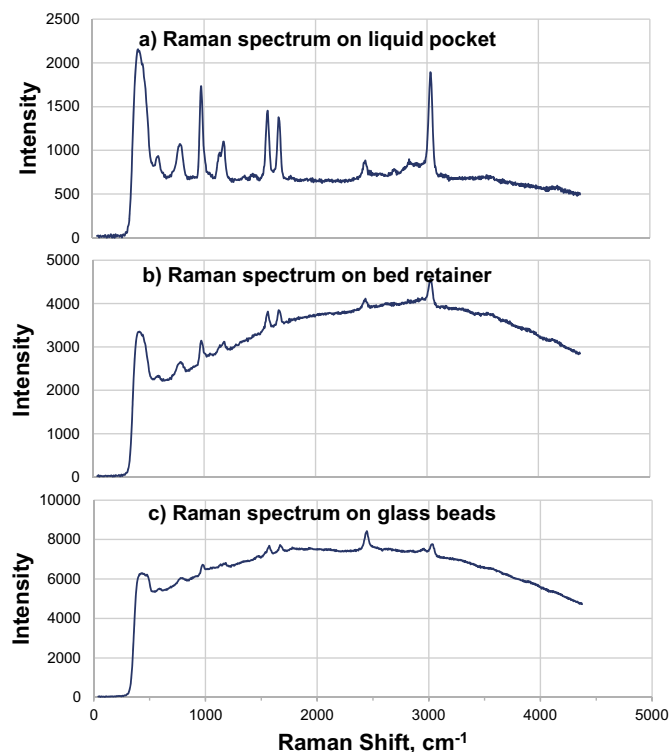


Fig. 3. Raman spectra obtained by focusing on a) liquid pocket, b) bed retainer and c) glass beads.

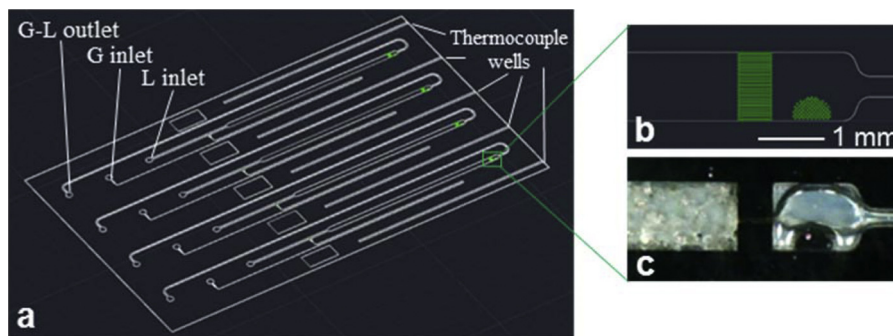


Fig. 4. a) Schematic of the micro-packed bed multi-microreactor chip, b) Details of the semi-circular pillar array for Raman sampling c) Picture of the same area as b) during gas-liquid flow over a bed of glass beads.

channel was 0.4 mm in width and was also used for catalyst packing. The width of the gas inlet channel was 20 μm and was determined based on pressure drop considerations so that the pressure drop over the gas inlet channel was at least two times larger than that over the catalyst bed at a reaction channel depth of 0.3 mm, to prevent liquid backflow into the gas channel. Five thermocouple wells were arranged alongside the reaction channels allowing for on-chip temperature measurement using thermocouples (K-type, 0.25 mm in diameter, Omega Engineering).

The multi-microreactor chip was fabricated by photolithography and deep reactive ion etching (DRIE) on 4" silicon wafers. The structured wafer was sealed with a Corning 7740 glass wafer (1.5 mm thick, with holes pre-drilled as inlets and outlets) through anodic bonding. For more details of the fabrication process see [33].

2.3. Reactor assembly

The bonded reactor chip was assembled with two custom-made housing parts: an inlet/outlet connector and a heating-clamping unit. The inlet/outlet connector consisted of a stainless steel chuck.

The top part of the chuck was interfaced with standard 1/16 in. coned compression fittings on the top side and had through holes and O-ring grooves on the other side. The through holes were aligned with the holes on the glass cover of the microreactor with O-rings (size 005, Perlast G80A, O-Rings Inc.) fitted into the grooves. The compression seal against the glass-silicon microreactor was formed by screwing the top chuck to the bottom of the connection chuck. The reaction zone heating was through a heating chuck that was machined to allow six resistive cartridge heaters (CIR-1021/120 V, Omega Engineering) to be inserted. A 0.7 mm \times 0.7 mm groove was machined over the middle of the heating chuck to enable a K-type thermocouple (Omega Engineering) to be inserted and contact both the reactor and the heating chuck. A 4 mm quartz plate was placed on top of the microreactor for improving heat insulation. A Π -shaped clamp was used to fix the quartz plate and the microreactor onto the heating chuck. A temperature controller was used to provide feedback control to the cartridge heaters. Using this heating system, reaction temperature of 25–250 $^{\circ}\text{C}$ can be achieved although the reaction experiments were carried out at 120 $^{\circ}\text{C}$.

2.4. Analytical methods and sampling

Raman spectroscopic measurement was carried out using a Ventana-532 Raman spectrometer with 532 nm laser excitation. To track the oxidation of benzyl alcohol, the area ratio between the Raman peaks at 1700 cm^{-1} (C=O stretching of benzaldehyde) and 1000 cm^{-1} (symmetric ring breathing) was examined. The liquid samples from the separators could be collected manually for a desired collection time and analysed offline by gas chromatography (Agilent 6890 with FID and InnoWax column). Such GC analysis was found to be critically important for calibrating the Raman intensity data.

The reactor assembly was fixed onto an x-y motorised positioning stage (Prior Scientific) which was mounted on a mounting plate (Edmund Optics). The Raman fibre optic probe was fixed on a modified microscope coarse/fine focusing unit which was placed above the microreactor chip through a rod mounted onto the mounting plate (Fig. 1 inset). The beam was directed on to the liquid pockets by adjusting the positioning stage and the coarse/fine focusing knobs to optimise the signal to background ratio. Both the adjustment of the positioning stage and the spectra acquisition conditions were controlled using LabView.

3. Experimental section

3.1. Catalyst preparation

For the preparation of Au, Pd, Au-Pd, Pd-Pt, Au-Pt or Au-Pd-Pt catalysts supported on TiO_2 , aqueous solutions of PdCl_2 (Sigma Aldrich, acidified by dropwise addition of HCl) $\text{HAuCl}_4 \cdot 3\text{H}_2\text{O}$ (Sigma Aldrich) and $\text{H}_2\text{PtCl}_6 \cdot 6(\text{H}_2\text{O})$. (Sigma Aldrich) of the desired concentrations were prepared. Two methods were implemented to prepare the catalysts:

Standard Impregnation (SImp). The requisite amounts of the metal solutions were combined and titania was added to the solution under stirring, where additional water was added to achieve a paste-like consistency (total volume of metal solutions and water $\sim 2.5\text{ ml g}^{-1}$ catalyst). The resultant slurry was dried at 110°C for 16 h. The resultant powder was ground using a pestle and mortar and calcined (1 g, 6 inch boat) in static air at 400°C for 3 h at a ramp rate of $20^\circ\text{C min}^{-1}$.

Sol immobilisation (SI). Polyvinylalcohol (PVA) (1 wt% aqueous solution, Aldrich, MW = 10000, 80% hydrolysed) and a fresh aqueous solution of 0.1 M NaBH_4 were prepared. To a mixed aqueous solution of the metal precursors (total volume 600 ml g^{-1} catalyst), the required amount of a PVA solution was added (PVA/metals, 1.2 wt/wt). The solution of NaBH_4 was then added (NaBH_4 /metals, 5 mol/mole) to form a dark sol. After 30 min of sol generation, the colloid was immobilised by adding the TiO_2 (Degussa P25). The solution was adjusted to pH 1 by the dropwise addition of concentrated sulphuric acid. The solution was stirred for 1 h, filtered and dried (110°C , 16 h). The resultant powder was ground using a pestle and mortar.

The prepared catalysts were pelletized and then crushed and sieved to get fractions with particle size range of $53\text{--}63\ \mu\text{m}$.

3.2. Packing of the multi-reactor chip

Packing catalyst particles into the reactor channels was carried out using an inlet/outlet connector made of Perspex and a five-port manifold (Fig. S2). The microreactor chip was first mounted onto the connector. The central port on the manifold was connected to a vacuum pump (E2 M 1.5, Edwards) and the other four ports were connected to the outlet ports on the connector. The gas inlet ports were sealed using sealing tape. Catalysts were packed through the

liquid inlet ports using a $200\ \mu\text{l}$ pipette tip as a funnel to aid the packing. Glass beads ($63\text{--}73\ \mu\text{m}$ in diameter) were also packed into the microreaction channel before and after the catalyst to stabilize the bed and aid gas-liquid distribution.

3.3. Reaction experiment procedure

The optimal alignment of the Raman probe with the liquid pockets on the microreactor chip was carried out using a flow of benzyl alcohol (0.02 ml/min) and oxygen (1 ml/min). The coordinates of the liquid pockets and the parameters of the Raman acquisition (integration time 100 ms, accumulation number 4, sampling time between reactors 0.2 min, sampling time intervals 4–5 min, total sampling number 50–70) were then input into the Labview program. The gas and the liquid flow were set to the designated values and the reaction was initiated by switching on the heater and starting the Raman acquisition. The integration under the diagnostic peaks at 1000 cm^{-1} and 1700 cm^{-1} was performed by the Labview program and the calculated ratio of the peak areas was displayed. Typical reaction conditions for catalyst evaluation were 0.005 g catalyst , 0.008 ml/min of benzyl alcohol, 1 ml/min of O_2 , 120°C and 2 bar(g) of back pressure at reactor outlets.

3.4. Correlation of Raman spectra to benzaldehyde yield

It has been reported previously that Raman spectra can be affected by temperature, reactant flow rate and the composition of reaction mixture with effects on peak positions, width and area [34–36]. All of these could significantly influence the quantitative product analysis. For benzyl alcohol oxidation on TiO_2 supported Au/Pd/Pt catalysts, the main products found in the reaction mixture were benzaldehyde, toluene and water. An initial calibration using prepared mixtures of benzyl alcohol and benzaldehyde at room temperature and 120°C showed that the peak ratio decreased both with increasing temperature and with the concentration of benzaldehyde (Fig. S3). Further examining the effect of toluene and water indicated that the Raman peak ratios were not significantly affected at low concentrations of toluene and water (corresponding to low benzyl alcohol conversion). As higher toluene and water concentrations were obtained at higher conversion (e.g. $\sim 80\%$), the Raman peak ratio decreased by $\sim 3\%$ due to increased toluene content and increased by $\sim 14\%$ with water production (Table S1). It was expected that the calibration with mixtures obtained directly from the reactor could account for the effect of temperature and composition on Raman spectrum [37]. The following calibration procedure was adopted. Benzyl alcohol catalytic oxidation was conducted at the reaction temperature (120°C) to generate different benzaldehyde yields. Raman spectra were collected at the same conditions as liquid samples from the gas-liquid separators which were analysed by GC. The resulting Raman peak ratios were correlated with the actual yield measured by GC and a calibration curve was generated (Fig. S4). This calibration curve was then used to calculate the yield in real time from Raman spectra obtained during microreactor operation.

4. Results and discussion

4.1. Validation of the reactor

An experimental test designed to validate the system was carried out by using a $1\% \text{ AuPd/TiO}_2$ catalyst prepared by sol-immobilization in previous work [11]. Each microreactor channel was packed with 0.005 g of the same catalyst and the same amount of glass beads which formed a 2 mm long bed downstream and 6 mm long bed upstream of the catalyst bed. The oxidation reaction was performed under a benzyl alcohol flow rate of 0.005 ml/min

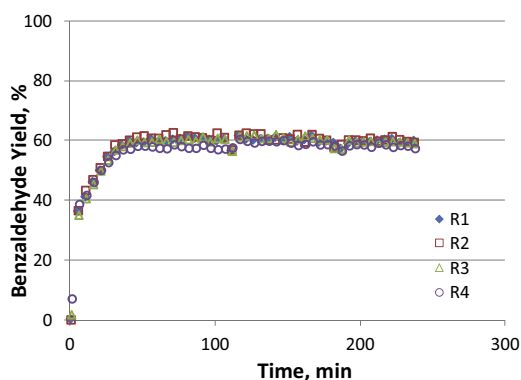


Fig. 5. Performance of the four microreactors (R1–R4) packed with the same catalyst (5 mg of 1% AuPd/TiO₂). Reaction conditions: benzyl alcohol 0.005 ml/min, oxygen 1 ml/min, 120 °C.

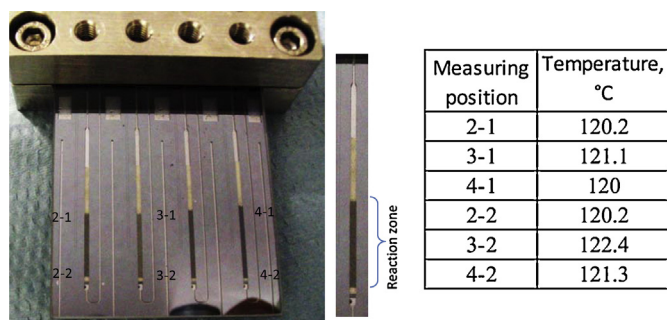


Fig. 6. Picture of the packed multichannel microreactor chip showing the thermocouple wells and the measured temperatures in the reaction zone when the heater was set at 120 °C.

Table 1
Metal content on TiO₂ support.

Catalyst	Metal content on TiO ₂ , wt%		
	Au	Pd	Pt
Au	1	-	-
Pd	-	1	-
Pt	-	-	1
AuPd	0.5	0.5	-
AuPt	0.5	-	0.1
PdPt	-	0.5	0.1
AuPdPt	0.5	0.5	0.1

and oxygen flow rate of 1 ml/min. Raman spectrum acquisition was started while the reactor temperature was rising from room temperature to 120 °C in 20 min. The on-stream yields of benzaldehyde calculated from the Raman peak ratios for the four reactors are shown in Fig. 5. It can be seen that the observed yields of benzaldehyde from the four reactors were very close; the maximum difference between the reactors was <5%.

The temperature of the chip at the reaction conditions was measured using three thermocouples inserted into the thermocouple wells located at the middle and the sides of the reactor chip, as shown in Fig. 6. The temperature deviation within the reaction zone was ~1 °C. These tests showed acceptable temperature uniformity throughout the reaction zone and consistent reaction performance over the four-reactor chip.

4.2. Catalyst evaluation

Fourteen catalysts were prepared on TiO₂ support using both SImp and SI methods with different metal content shown in Table 1.

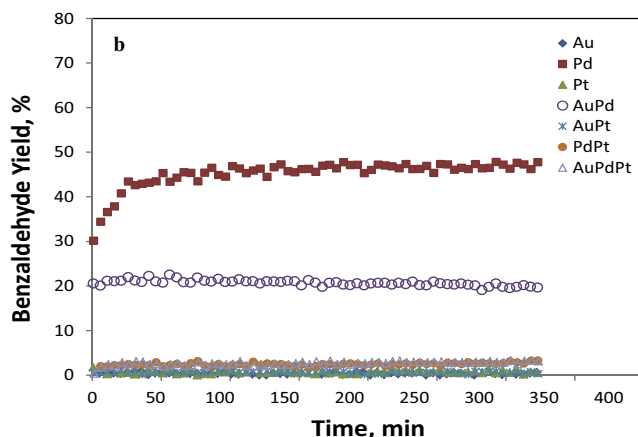
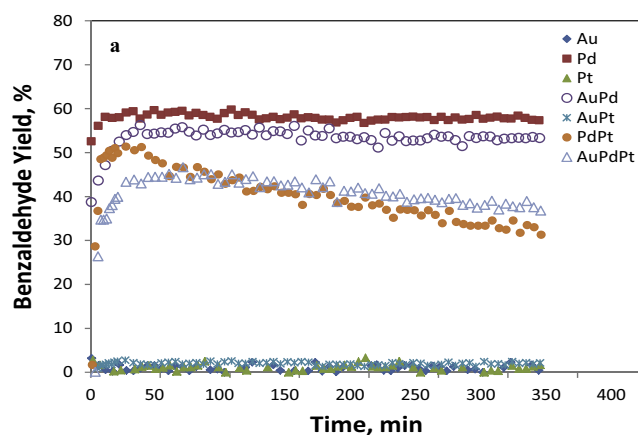


Fig. 7. Time-on-stream yield of benzaldehyde from Raman spectroscopic measurement for the catalysts prepared by a) sol-immobilization and b) standard impregnation. Reaction conditions: catalyst 5 mg, benzyl alcohol 0.005 ml/min, oxygen 1 ml/min, 120 °C.

Four reaction experiments were carried out to evaluate the fourteen catalysts.

Fig. 7a shows the time-on-stream yield of benzaldehyde analysed by Raman spectroscopy for the catalysts prepared by the SI method. Pd and AuPd catalysts showed quite stable activity over the 5-h reaction time, with yield of 58% and 53% respectively. The trimetallic AuPdPt catalyst showed a slight deactivation with yield decreasing from 44% to 38%, while the yield of the PdPt catalyst decreased more quickly from ~52% to 34%. It is interesting to notice that Au, Pt and AuPt catalysts showed very low yields (<3%) under the conditions investigated. The catalysts tested showed a catalytic activity sequence as: Pd > AuPd > AuPdPt > PdPt > (Au, Pt, AuPt).

The catalysts prepared by the SImp method showed the same catalytic activity sequence as those prepared by SI but with lower yields of benzaldehyde (Fig. 7b). Pd and AuPd catalysts again showed quite stable activity over the 5-h reaction time with yields of 46% and 21% respectively. Au, Pt and AuPt catalysts showed negligible activity. The yields from PdPt and AuPdPt catalysts were low around 3%.

Trimetallic (AuPdPt), bimetallic (AuPd, AuPt and PdPt) and monometallic (Au, Pd and Pt) catalysts supported on active carbon and TiO₂ prepared by sol-immobilisation and impregnation have been previously used in batch reactors and the fresh catalysts have been well characterised [32,38]. The trimetallic and bimetallic catalysts prepared by the sol-immobilisation method all have similar particle size distribution with mean diameters in the 2–3 nm range. The results from the batch reactor operated at 120 °C and 10 bar oxygen pressure with the catalysts prepared by the sol-immobilisation showed that the highest yield of benzalde-

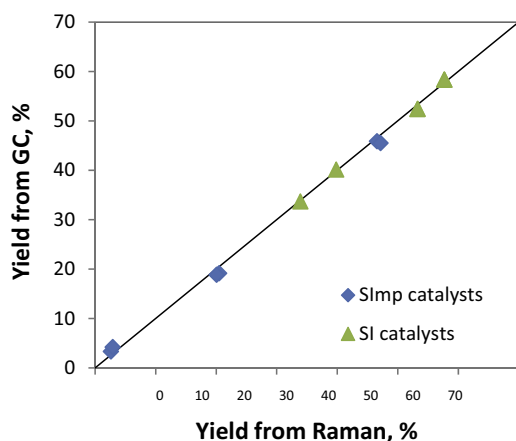


Fig. 8. Parity plot of yields from Raman spectroscopy and from GC analysis.

hyde was obtained from AuPd catalysts, the activity order followed the sequence AuPd > Pd > AuPdPt > PdPt > AuPt > Pt. The yields from AuPd, Pd and AuPdPt catalysts were over 40% (54.1, 44.3 and 43.2% respectively) while from PdPt, AuPt and Pt catalysts were relatively low (12.5, 8.2 and 2.5% respectively) [32]. The catalyst activity evaluated in the multichannel reactor showed a similar pattern (Fig. 7a) but with the Pd catalyst showing a slightly higher (~5%) yield than AuPd catalyst. This may be due to differences in oxidation state of Pd under flow reaction conditions and this is a factor that we will address in subsequent studies.

To cross check the Raman spectroscopy–yield calibration, liquid samples were collected and analysed by GC. Plotting the yields of benzaldehyde obtained from GC analysis versus those measured by Raman spectroscopy is shown in Fig. 8. The excellent agreement between the results from GC and Raman spectroscopy validates the calibration procedure employed and also demonstrates the accuracy of the online Raman analysis.

The results presented above show that using the micropacked-bed reactor platform developed enables the implementation of a convenient fibre-optic Raman spectroscopic evaluation and provides an efficient way to monitor the activity and stability of catalysts. The information generated can be used as guidance for further investigating the effect of composition of catalysts and optimising their preparation method for improving their performance.

5. Conclusions

A carefully designed micropacked-bed multi-reactor chip was designed to facilitate the application of a portable Raman spectrometer for on-chip monitoring of catalytic gas/liquid/solid reaction. Liquid pockets were engineered at the outlet of the four packed beds, in order to permit efficient application of fibre optic Raman excitation and collection of spectra for reaction mixture analysis. Using the oxidation of benzyl alcohol as a model reaction, the effect of temperature and composition of reaction mixtures on Raman spectra could be accounted for by calibration using gas chromatography of samples obtained directly from the reactors. Fourteen catalysts containing different combinations of Au, Pd and Pt supported on TiO₂ prepared by standard impregnation (SImp) and sol-immobilization (SI) methods were tested. Pd and AuPd catalysts prepared by SI showed good activity and stability, while the PdPt and AuPdPt catalysts were less active and stable than Pd and AuPd catalysts. The activity sequence for the catalysts prepared by SI was Pd > AuPd > AuPdPt > PdPt > (Au, Pt and AuPt). The catalysts prepared by SImp showed the same activity sequence but were overall less active than those prepared by SI. The results demonstrated that the developed platform is suitable for efficiently assessing catalyst

stability and activity in gas/liquid/solid reactions, provided that the reaction system is sensitive to Raman measurement.

Acknowledgements

Funding for this work from EPSRC, UK (grants EP/J017833/1, EP/J017868/1, EP/L027240/1) is gratefully acknowledged. We also thank the London Centre for Nanotechnology and in particular Steve Etienne for his support in the fabrication of microreactors.

Appendix A. Supplementary data

Supplementary data associated with this article can be found, in the online version, at <http://dx.doi.org/10.1016/j.cattod.2016.06.007>.

References

- [1] K. Jähnisch, V. Hessel, H. Löwe, M. Baerns, *Angew. Chem. Int. Ed.* 43 (2004) 406–446.
- [2] P.L. Mills, D.J. Quiram, J.F. Ryley, *Chem. Eng. Sci.* 62 (2007) 6992–7010.
- [3] R.L. Hartman, K.F. Jensen, *Lab Chip* 9 (2009) 2495–2507.
- [4] K.F. Jensen, *Chem. Eng. Sci.* 56 (2001) 293–303.
- [5] W. Ferstl, T. Klahn, W. Schweikert, G. Billbe, M. Schwarzer, S. Loebbecke, *Chem. Eng. Technol.* 30 (2007) 370–378.
- [6] J.P. McMullen, K.F. Jensen, *Annu. Rev. Anal. Chem.* (2010) 19–42.
- [7] S. Löbbecke, *Integration of sensors and process analytical techniques, in: Micro Process Engineering*, Wiley-VCH Verlag GmbH, 2008, pp. 249–266.
- [8] J. Yue, J.C. Schouten, T.A. Nijhuis, *Ind. Eng. Chem. Res.* 51 (2012) 14583–14609.
- [9] N. Al-Rifai, E. Cao, V. Dua, A. Gavriilidis, *Curr. Opin. Chem. Eng.* 2 (2013) 338–345.
- [10] E. Cao, S. Firth, P.F. McMillan, A. Gavriilidis, *Catal. Today* 126 (2007) 119–126.
- [11] E. Cao, M. Sankar, S. Firth, K.F. Lam, D. Bethell, D.K. Knight, G.J. Hutchings, P.F. McMillan, A. Gavriilidis, *Chem. Eng. J.* 167 (2011) 734–743.
- [12] A. Urakawa, F. Trachsel, P.R. von Rohr, A. Baiker, *Analyst* 133 (2008) 1352–1354.
- [13] P. Beato, R. Kraehnert, S. Engelschalt, T. Frank, R. Schlögl, *Chem. Eng. J.* 135 (Supplement 1) (2008) S247–S253.
- [14] C.K.C. Tan, W.N. Delgass, C.D. Baertsch, *Appl. Catal. B: Environ.* 93 (2009) 66–74.
- [15] C. Daniel, M.O. Clarté, S.P. Teh, O. Thinin, H. Provendier, A.C. Van Veen, B.J. Beccard, Y. Schuurman, C. Mirodatos, *J. Catal.* 272 (2010) 55–64.
- [16] J.-D. Grunwaldt, B. Clausen, *Top. Catal.* 18 (2002) 37–43.
- [17] S. Baier, A. Rochet, G. Hofmann, M. Kraut, J.D. Grunwaldt, *Rev. Sci. Instrum.* 86 (2015).
- [18] G. Sankar, E. Cao, A. Gavriilidis, *Catal. Today* 125 (2007) 24–28.
- [19] J.-D. Grunwaldt, B. Kimmerle, S. Hannemann, A. Baiker, P. Boye, C.G. Schroer, *J. Mater. Chem.* 17 (2007) 2603–2606.
- [20] D. Farrusseng, *Surf. Sci. Rep.* 63 (2008) 487–513.
- [21] Z.Q. Zheng, X.P. Zhou, *Comb. Chem. High Throughput Screening* 14 (2011) 147–159.
- [22] U. Rodemerck, D. Wolf, O.V. Buyevskaya, P. Claus, S. Senkan, M. Baerns, *Chem. Eng. J.* 82 (2001) 3–11.
- [23] J. Pérez-Ramírez, R.J. Berger, G. Mul, F. Kapteijn, J.A. Moulijn, *Catal. Today* 60 (2000) 93–109.
- [24] J.A. Kapteijn, J. Moulijn, *Laboratory reactors, in: Handbook of Heterogeneous Catalysis*, Wiley-VCH Verlag GmbH, 2008, pp. 1359–1398.
- [25] G. Li, D. Hu, G. Xia, J.M. White, C. Zhang, *Rev. Sci. Instrum.* 79 (2008) 074101.
- [26] G. Li, D. Hu, G. Xia, Z. Conrad Zhang, *Top. Catal.* 52 (2009) 1381–1387.
- [27] M. García-Casado, J. Prieto, E. Vico-Ruiz, E. Lozano-Diz, C. Goberna-Selma, M.A. Bañares, *Appl. Spectrosc.* 68 (2014) 69–78.
- [28] D.I. Enache, J.K. Edwards, P. Landon, B. Solsona-Espriu, A.F. Carley, A.A. Herzing, M. Watanabe, C.J. Kiely, D.W. Knight, G.J. Hutchings, *Science* 311 (2006) 362–365.
- [29] N. Dimitratos, J.A. Lopez-Sanchez, D. Morgan, A.F. Carley, R. Tiruvalam, C.J. Kiely, D. Bethell, G.J. Hutchings, *PCCP* 11 (2009) 5142–5153.
- [30] P. Miedziak, M. Sankar, N. Dimitratos, J.A. Lopez-Sanchez, A.F. Carley, D.W. Knight, S.H. Taylor, C.J. Kiely, G.J. Hutchings, *Catal. Today* 164 (2011) 315–319.
- [31] M. Sankar, E. Nowicka, R. Tiruvalam, Q. He, S.H. Taylor, C.J. Kiely, D. Bethell, D.W. Knight, G.J. Hutchings, *Chem. Eur. J.* 17 (2011) 6524–6532.
- [32] Q. He, P.J. Miedziak, L. Kesavan, N. Dimitratos, M. Sankar, J.A. Lopez-Sanchez, M.M. Forde, J.K. Edwards, D.W. Knight, S.H. Taylor, C.J. Kiely, G.J. Hutchings, *Faraday Discuss.* 162 (2013) 365–378.
- [33] E. Cao, A. Gavriilidis, *Catal. Today* 110 (2005) 154–163.
- [34] S. Mozharov, A. Nordon, D. Littlejohn, C. Wiles, P. Watts, P. Dallin, J.M. Girkin, *J. Am. Chem. Soc.* 133 (2011) 3601–3608.
- [35] C. Fräulin, G. Rinke, R. Dittmeyer, *J. Flow Chem.* 3 (2013) 87–91.
- [36] M.J. Pelletier, *Appl. Spectrosc.* 53 (1999) 1087–1096.
- [37] R.A. Skilton, A.J. Parrott, M.W. George, M. Poliakoff, R.A. Bourne, *Appl. Spectrosc.* 67 (2013) 1127–1131.
- [38] G.J. Hutchings, C.J. Kiely, *Acc. Chem. Res.* 46 (2013) 1759–1772.